



Molecular Crystals and Liquid Crystals

Publication details, including instructions for authors and subscription information:
<http://www.tandfonline.com/loi/gmcl16>

Carbonate Schiff Base Nematic Liquid Crystals: Synthesis and Electro-optic Properties

M. J. Rafuse^a & R. A. Soref^a

^a Sperry Rand Research Center, 100 North Road, Sudbury, Mass, 01776
Version of record first published: 21 Mar 2007.

To cite this article: M. J. Rafuse & R. A. Soref (1972): Carbonate Schiff Base Nematic Liquid Crystals: Synthesis and Electro-optic Properties, *Molecular Crystals and Liquid Crystals*, 18:2, 95-104

To link to this article: <http://dx.doi.org/10.1080/15421407208083253>

PLEASE SCROLL DOWN FOR ARTICLE

Full terms and conditions of use: <http://www.tandfonline.com/page/terms-and-conditions>

This article may be used for research, teaching, and private study purposes. Any substantial or systematic reproduction, redistribution, reselling, loan, sub-licensing, systematic supply, or distribution in any form to anyone is expressly forbidden.

The publisher does not give any warranty express or implied or make any representation that the contents will be complete or accurate or up to date. The accuracy of any instructions, formulae, and drug doses should be independently verified with primary sources. The publisher shall not be liable for any loss, actions, claims, proceedings, demand, or costs or damages whatsoever or howsoever caused arising directly or indirectly in connection with or arising out of the use of this material.

Carbonate Schiff Base Nematic Liquid Crystals: Synthesis and Electro-optic Properties

M. J. RAFUSE and R. A. SOREF

Sperry Rand Research Center
100 North Road
Sudbury, Mass. 01776

Received November 18, 1971

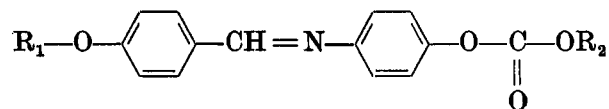
Abstract—Two new series of nematic Schiff base liquid crystals, methyl *p*-alkoxybenzylidene *p*-aminophenyl carbonates and alkyl *p*-anisylidene *p*-aminophenyl carbonates were synthesized. Preparative methods and transition-point data are given. Electro-optic measurements show the alkyl *p*-anisylidene *p*-aminophenyl carbonates to possess a negative dielectric anisotropy and to exhibit dynamic scattering preceded by classical domain formation at 6–10 V rms. In contrast, the methyl carbonates have a positive dielectric anisotropy, and in samples where the nematic alignment is initially parallel to the electrodes, the liquid crystal has a dielectric realignment threshold at 5–10 V rms, above which the nematic layer tends towards the homeotropic state.

1. Introduction

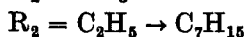
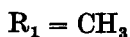
One current emphasis in the liquid crystal field has been to obtain nematics with wide temperature ranges, extending above and below room temperature, for display applications. The only well-known single component nematic liquid crystal that exists at room temperature is *p*-methoxybenzylidene *p*-*n*-butylaniline.⁽¹⁾ However, a room temperature mesophase range having useful electro-optic properties has often been achieved by mixing higher temperature nematics.

The purpose of this paper is to describe two novel series of Schiff base nematics that have reduced crystalline-to-nematic points in binary and ternary systems. These compounds are similar in molecular structure to the known and electro-optically useful *p*-alkoxybenzylidene *p*-aminophenyl acylates.⁽²⁾ They differ in that

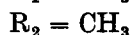
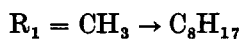
the acylate moiety is replaced with a carbonate group to give the following two series labelled *A* and *B*:



Series A



Series B



2. Preparation

The alkoxybenzaldehydes, where not commercially available, were prepared by etherification of *p*-hydroxybenzaldehyde with the appropriate alkyl iodide. The phenolic Schiff bases were obtained by the condensation of the appropriate *p*-alkoxybenzaldehyde with *p*-aminophenol. The carbonates were prepared by treatment of the phenolic Schiff base with the appropriate alkyl chloroformate in basic solution. Reagent grade chemicals were used throughout without further purification except where noted, and were identified by infrared spectra and, where possible, by melting point. Analyses were performed only on the end product liquid crystals by Galbraith Laboratories and agreed with calculated values to $\pm 0.3\%$. Nuclear magnetic resonance spectra were run by Sadtler Laboratories. Typical synthetic procedures are as follows:

p-*iso*-Pentoxybenzaldehyde was prepared according to the procedure of Weygand and Gabler³ by refluxing *p*-hydroxybenzaldehyde (10.6 g; 0.087 mole) and 1-iodo-3-methylbutane (19.8 g; 0.1 mole) in 50 cc dry methanol containing 6 g KOH for 48 hours under nitrogen. Distillation of the neutralized ether extract gave 8.94 g (53% yield) *p*-*iso*-pentoxybenzaldehyde bp_{0.01 mm} 80–2°C; ir_{CCl_4} 2845, 2735, 1700 cm^{-1} (HC=O).

p-*n*-Butoxybenzylidene *p*-aminophenol: The condensation of *p*-*n*-butoxybenzaldehyde (8.9 g; 0.05 mole) and *p*-aminophenol (5.5 g; 0.05 mole) in dry ethanol gave 13 g (91% yield) *p*-*n*-butoxybenzylidene *p*-aminophenol mp 152–3°C; ir_{nujol} 3300–2400 (OH), 1600 cm^{-1} (—C=N—), no C=O.

n-Heptyl *p*-anisylidene *p*-aminophenyl carbonate: To *p*-anisylidene *p*-aminophenol (2.3 g; 0.01 mole) in 20 ml dry pyridine, distilled

from BaO, containing 2.1 g (0.02 mole) triethylamine was added dropwise with stirring *n*-heptylchloroformate (3.58 g; 0.02 mole). After 4 hours at room temperature, water was added and the aqueous reaction mixture extracted with benzene. Evaporation of the benzene layer followed by recrystallization from ethanol, then hexane, yielded 3.12 g (84% yield) **7**, mp (40) 75–7 °C nem.; ir_{CCl_4} 1765 (C=O) 1600 cm^{-1} (—HC=N—); anal. calc. for $\text{C}_{22}\text{H}_{29}\text{NO}_4$: C—71.52, H—7.37, N—3.79; found C—71.44, H—7.56, N—3.64.

Methyl p-hexoxybenzylidene p-aminophenyl carbonate: To *p*-*n*-hexoxybenzylidene *p*-aminophenol (6.0 g; 0.02 mole), mp 150–1 °C, prepared from purified E.K. *p*-hexoxybenzaldehyde, in 20 ml pyridine (distilled from BaO) and 4.2 g triethylamine was added dropwise with stirring methyl chloroformate (3.8 g; 0.04 mole) in 25 ml dry benzene. After stirring 2.5 hours at room temperature, the reaction mixture was flooded with water and extracted with benzene. After evaporation, a solid residue was formed. Fractional recrystallization from ethanol and then hexane gave a constant melting point mixture of **14** with *p*-*n*-hexoxybenzylidene *p*-aminophenol, mp 88 °C (63 : 37% by NMR), and 1.46 g (21% yield) **14**, mp 67–113 °C, nem.; ir_{CCl_4} 1765 (C=O), 1600 cm^{-1} (C=N), no O—H or N—H; anal. calc. for $\text{C}_{21}\text{H}_{25}\text{NO}_4$: C—70.96, H—7.09, N—3.94; found C—71.21, H—7.07, N—4.16

3. Measurement Procedure

All transition temperatures were measured in capillary tubes in a Mel-Temp apparatus and then observed through a Bausch and Lomb polarizing microscope in both heating and cooling cycles on a Koffler hot stage. All transition temperatures are corrected.

To observe electro-optic response, the liquid crystal materials were placed in parallel-plate sample cells having transparent electrodes. The electrodes consisted of indium-oxide coating on flat glass plates (Nesatron⁽⁴⁾). Teflon⁽⁶⁾ shims between the plates maintained a uniform plate separation of $13\text{ }\mu$. Two edges of the sample cell were sealed with epoxy and electrical lead-ins were attached with silver epoxy. The liquid crystal compound in powder form was placed at an open edge of the cell while the cell was heated to about 100 °C. The compound melted and flowed into the half-

sealed cell, giving a nematic layer $13\ \mu$ thick. The optical characteristics of the sample in its nematic phase were observed through a polarizing microscope while the sample was kept at a constant temperature on the hot stage. At the same time, the sample cell was excited with a steady sinusoidal ac electric field in the 5 to 20,000 Hz range. Then the measurements were repeated with dc electrical excitation. The resistivity of the liquid crystals tested ranged from 2×10^8 to 4×10^9 Ohm cm.

4. Results and Discussion

Thermal Behavior: All of the Series A and B samples that were prepared exhibited liquid crystal phases. The transition temperatures for these compounds are given in Table 1. The variation of transition

TABLE 1 Transition Temperatures for Carbonate Schiff Bases Prepared for This Study

No.	R_1	R_2	Transition temperatures ($^{\circ}\text{C}$)		
			C-Sm	Sm-Nem ^(a)	Nem-Iso
1	CH_3	CH_3		(45) ^(b) 88	109
2	C_2H_5	CH_3		(52) 88	134
3	$n\text{-C}_3\text{H}_7$	CH_3		(64) 99	108
4	$n\text{-C}_4\text{H}_9$	CH_3		(58) 75	114
5	$n\text{-C}_5\text{H}_{11}$	CH_3		(59) 89	102
6	$iso\text{-C}_5\text{H}_{11}$	CH_3		(50) 78	85
7	$n\text{-C}_6\text{H}_{13}$	CH_3	(45) ^(c)	(69) ^(d) 87 ^(e)	113
8	$n\text{-C}_7\text{H}_{15}$	CH_3	(36)	(77) 84	106
9	CH_3	C_2H_5		(39) 82	102
10	CH_3	$n\text{-C}_3\text{H}_7$		(43) 78	87
11	CH_3	$n\text{-C}_4\text{H}_9$		(23) 68	87
12	CH_3	$n\text{-C}_5\text{H}_{11}$		(27) 47	82
13	CH_3	$n\text{-C}_6\text{H}_{13}$		(29) 67	78
14	CH_3	$n\text{-C}_7\text{H}_{15}$		(40) 75	78
15	CH_3	$n\text{-C}_8\text{H}_{17}$		(50) 75	77

(a) If there is no smectic phase, then this is the crystal to nematic transition temperature. Temperatures in parentheses were obtained on cooling.

(b) Monotropic nematic phase obtained on the cooling run.

(c) Monotropic smectic phase obtained on the cooling run.

(d) Two monotropic smectic phases were noted, with a transition from Smectic I to Smectic II at 59°C .

(e) Only compound 7 did not exhibit a monotropic nematic liquid crystal phase.

temperatures with increasing chain length for Series *B* (1–8) is shown in Fig. 1. The similarity of the transition temperatures to those for the corresponding acetates^(2,6) particularly in the nematic–isotropic transition, can be seen. Figure 1 shows that the usual behavior of an homologous series is followed, namely alternation of transition temperatures with increasing chain length, attributed to the “cog-wheel” conformation of the alkyl chain.⁽⁷⁾ As with many other homologous series of liquid crystals, early members show nematic character and later ones show smectic, albeit monotropic, character.

Series *A* (9–15) on the other hand, in which the carbonate alkyl chain length is varied, has a transition temperature vs chain length behavior, as shown in Fig. 2, that does not follow the odd-even alternation attributed to “cog-wheel” conformation. There is no

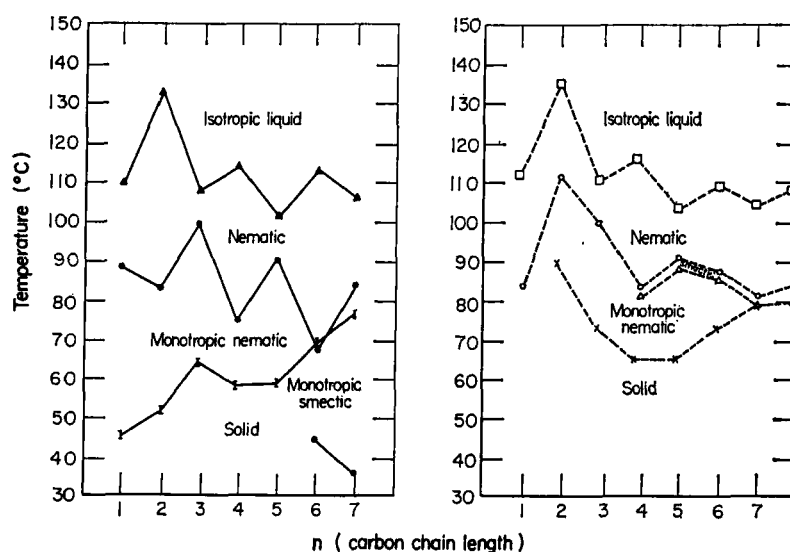
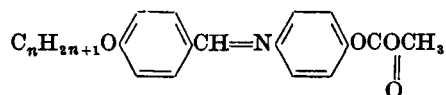
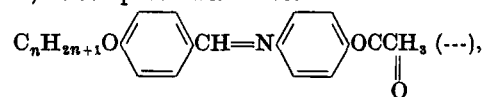


Figure 1. Variation of transition temperatures with chain length for



Series *B* (—) as compared with those for the acetates



taken from Refs. 2 and 6.

reason to assume that the alkyl group in the carbonate chain does not follow the same geometry as the alkyl group in Series *B*. Rather it appears that the influence of the carbonate group itself dominates over any contribution from the cog-wheel conformation of the carbon chain. As seen in Fig. 2, although the nematic phase has decreased substantially in thermal stability when $R_2 = C_7H_{15}$ and C_8H_{17} , no smectic phase, even monotropic, was observed. Following Gray's theory⁽⁷⁾ concerning molecular requirements for liquid crystal behavior, in Series *A* the mesophase-forming attractions are largely terminal with dispersive forces becoming more important with longer carbonate chain lengths. If, as Gray points out, a predominance of lateral attractions is instrumental in allowing the formation of a smectic phase, the carbonates listed in Fig. 2 have weak lateral attractions. With increasing chain length and the accompanying fall-off of terminal attractions, the nematic stability fades without the usual inception of a smectic phase (Fig. 2). This indicates either that the carbonate group does not contribute a strong cross-axis dipole or that it is shielded from close approach to other dipoles

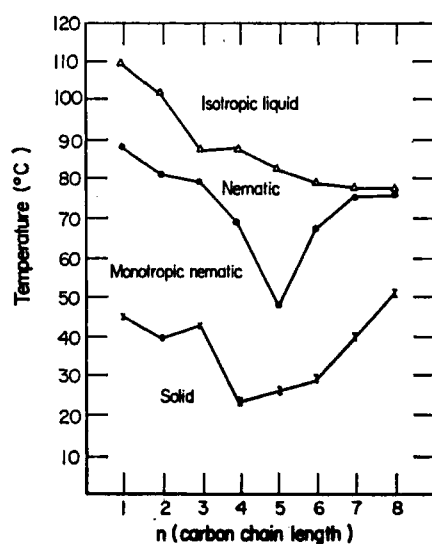
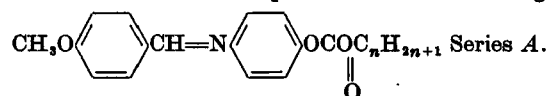


Figure 2. Variation of transition temperatures with chain length for



by the long alkyl chain. By analogy with the ether Schiff bases, the latter possibility does not seem likely.

Electrical Behavior: In an electric field, the compounds in Series A (9–15) exhibited hydrodynamic instabilities.^(8,9) They became turbulent or “dynamic scattering”⁽⁸⁾ throughout their nematic range under the influence of 10 to 15 V dc, preceded by the formation of Williams’ stripe domains⁽¹⁰⁾ at 6 to 10 V dc. For ac drive, the dynamic scattering threshold increased with increasing drive frequency, rising rapidly at a critical frequency, f_c , of 50 to 100 Hz.

In our experiments, the molecular alignment of the nematic layer was homogeneous, that is, the long axes of the molecules were oriented parallel to the electrode surfaces. This molecular texture, seen in transmission between crossed optical polarizers, appears “white”. Using the crossed-polarizer set-up, this texture was observed in two voltage ranges: from zero voltage to the domain voltage for $f < f_c$, and from zero to 50 Vrms for $f > f_c$. In both cases, the texture was stable and did not darken.

The stability of the homogeneous texture in an electric field applied normal to the axes, and the occurrence of conventional dynamic scattering, imply that the Series A nematics have negative dielectric anisotropy ($\epsilon_{\parallel} - \epsilon_{\perp} < 0$).⁽¹¹⁾

The Series B compounds behaved differently. They exhibited dielectric reorientation, commencing at a threshold of 4 to 8 V rms at frequencies from 5 to several thousand hertz. Through crossed polarizers, the observed color of the Series B sample changed with increasing voltage from threshold to about 20 V rms, followed by darkening from 20 to 50 V rms. In other words, the nematic layer went from a homogeneous to a “hemi-homeotropic” or half-dark texture. This indicates that molecules initially parallel to the electrode surfaces were caused to realign almost perpendicular to those surfaces. That the sample went only half-dark is the result of the nematic having reached a stable alignment with its optic axis not quite perpendicular to the electrode surfaces.

The Series B compounds also exhibited weak turbulence at frequencies below 100 Hz for applied voltages in the 20 to 75 V rms range. This turbulence was “nucleated”, that is, it took place in small, separated areas and resembled boiling from a point source. It was not preceded by domain formation at lower voltages. There was

a small amount of optical scattering associated with the turbulence and the optical transmission of the samples decreased slightly when they were turbulent.

At dc, the lower alkoxyis, 1–5, exhibited a more densely packed turbulence when subjected to 11 V or more. However, the higher homologs 7 and 8, showed dielectric reorientation at dc without the onset of turbulence.

Figure 3 summarizes the electro-optic behavior of the Series *B* nematics and shows the frequency dependence of two thresholds for a typical Series *B* compound, these being the dielectric reorientation threshold and the nucleated-turbulence threshold. The figure also illustrates the molecular response in the various frequency-voltage regimes.

The field-induced transition from homogeneous to hemi-homeotropic alignment, described above, is a clear indication that the Series *B* methyl carbonates (1–8) have a positive dielectric anisotropy ($\epsilon_{\parallel} - \epsilon_{\perp} > 0$), unlike (9–15). Assuming this, the voltage-frequency

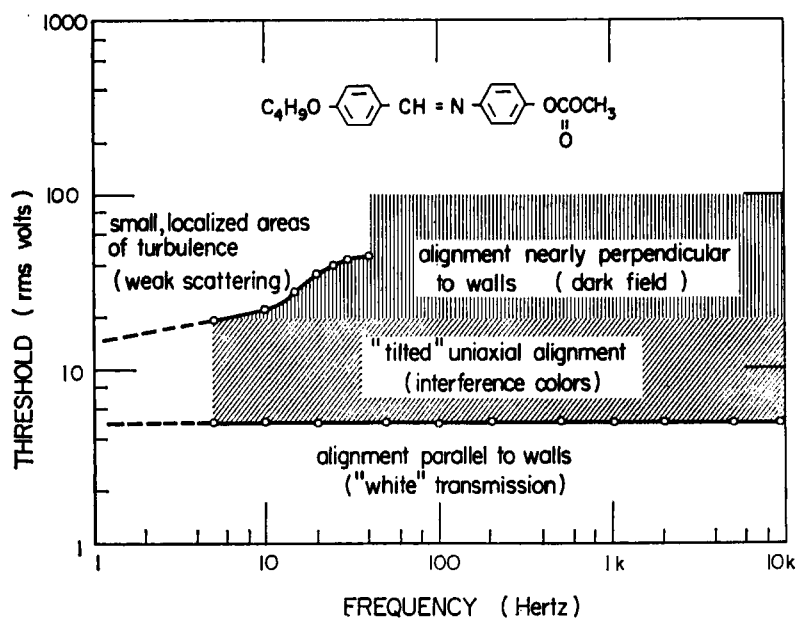


Figure 3. Threshold for electro-optic response vs. frequency of applied voltage for a representative Series *B* nematic liquid crystal at $T = 100^{\circ}\text{C}$. Initial ordering of molecular axis was parallel to the electrodes.

diagram of Fig. 3 is complementary to the diagram given in Ref. 11 (Fig. 7) for a negative-anisotropy nematic. Both diagrams show a dielectric reorientation (Fredericksz transition) occurring at voltages below the hydrodynamic instability threshold.

Previously, only molecules with strong on-axis dipoles, such as *p*-ethoxybenzylidene-*p*-aminobenzonitrile,⁽¹²⁾ have been shown to possess positive dielectric anisotropy. In the Series *B* compounds, the existence of a strong, on-axis, permanent dipole moment is not obvious from an examination of the molecular structure. Therefore, using the on-axis criterion, a satisfactory explanation for the positive anisotropy cannot be offered at this time.

5. Summary

Two new series of Schiff base nematic liquid crystals which behave differently in their thermal and electro-optical properties have been prepared and examined. In the transition-temperature measurements, the carbonates with increasing carbonate alkyl chains do not show the influence of "cog-wheel" conformation as do the carbonates with increasing alkoxy chains. In an applied electric field, the methyl carbonates with increasing alkoxy chain length exhibit dielectric reorientation from a spontaneous homogeneous alignment to a hemi-homeotropic alignment, indicating a positive dielectric anisotropy. The alkyl carbonates exhibit domain formation and turbulence in an ac or dc field, with no realignment of the initial homogeneous texture, indicating a negative dielectric anisotropy.

REFERENCES

1. Jones, D., Creagh, L. and Lu, S., *Appl. Phys. Letters* **16**, 61 (1970).
2. Goldmacher, J. E. and Castellano, J. A., Brit. Pat. 1,170,486, Nov. 12, 1969.
3. Weygand, C. and Gabler, R., *J. Prakt. Chem.* **151**, 215 (1938).
4. Trademark of PPG Industries.
5. Trademark of E. I. DuPont de Nemours & Co., Inc.
6. Unpublished work, this laboratory.
7. Gray, G. W., *Molecular Structure and the Properties of Liquid Crystals*, Academic Press., New York (1962).
8. Heilmeyer, G. H., Zannoni, J. A. and Barton, L. A., *Proc. IEEE* **56**, 1162 (1968).

9. Orsay Liquid Crystal Group, A.C. and D.C. Regimes in the Electrohydrodynamical Instabilities of a Nematic Liquid Crystal, Third International Liquid Crystal Conference, Berlin, August 24–28, 1970.
10. Williams, R., *J. Chem. Phys.* **39**, 384 (1960).
11. Soref, R. A. and Rafuse, M. J., *J. Applied Phys.*, to be published May 1972.
12. Heilmeyer, G. H., Castellano, J. A. and Zanoni, L. A., *Mol. Cryst. and Liq. Cryst.* **8**, 293–304 (1969).